Materials Characterization 121 (2016) 195–198

Contents lists available at ScienceDirect

Materials Characterization

journal homepage: www.elsevier.com/locate/matchar

Structural and compositional evolution of $Al_3(Zr,Y)$ precipitates in Al-Zr-Y alloy

Haiyan Gao [a,b], Wuqiang Feng [a], Yufei Wang [a], Jing Gu [a], Yongzhi Zhang [a], Jun Wang [a,b,*], Baode Sun [a,b]

[a] State Key Laboratory of Metal Matrix Composites, Shanghai Jiao Tong University, Shanghai 200240, China
[b] Shanghai Key Laboratory of Advanced High-temperature Materials and Precision Forming, Shanghai 200240, China

ARTICLE INFO

Article history:
Received 25 June 2016
Received in revised form 6 October 2016
Accepted 9 October 2016
Available online 11 October 2016

Keywords:
Al-Zr-Y
Atom probe
Nucleation
Precipitation evolution
Binding energy

ABSTRACT

Structural and compositional evolution of $Al_3(Zr,Y)$ precipitates in aged Al-Zr-Y alloy was investigated through atom probe tomography (APT) **and t**ransmission electron microscope (TEM) analysis and first principles calculations. The results show that short-bar-shaped $D0_{19}$-Al_3Y with some Zr atoms dissolved in precipitated at the very beginning of decomposition and worked as heterogeneous nuclei for $L1_2$-Al_3Zr with spherical morphology **af**ter being aged at 400 °**C for** 2 **h**. Quasi-static coarsening happened as the aging treatment lasted from 2 h to 200 h. However, distribution of Zr and Y atoms in $Al_3(Zr,Y)$ is nearly uniform and $Al_3(Zr,Y)$ do not have the typical "Al_3RE core-Al_3Zr shell" structure which observed in other RE containing Al-Zr-RE alloys with $L1_2$-Al_3RE as nuclei. First principles calculations revealed that binding energy between Y and Zr is strong during the growth of $Al_3(Zr,Y)$, which led to the co-precipitation of Y and Zr atoms and attribute to the evolution of $Al_3(Zr,Y)$.

1. Introduction

Dilute Al-Zr alloys find wide applications at elevated temperatures because $L1_2$-Al_3Zr precipitated during aging of Al-Zr alloy is coherent with α-Al matrix and kinetically stable up to ~475 °C [1]. However, Al_3Zr precipitates are always in a low number density. Due to microsegregation of Zr during solidification, precipitates free zone (PFZ) always formed at the grain boundaries and inter-dendrite regions, which often became the original place for recrystallization [2]. The combined additions of Rear Earth (RE) elements, such as Sc, Yb, Er, with Zr lead to formation of $L1_2$-Al_3RE in the early stage of decomposition and act as nucleus for $L1_2$-Al_3Zr due to different diffusion coefficient of RE and Zr in Al matrix [3–8]. Attractive properties of the precipitates, such as larger number density, higher recrystallization temperature and reduced coarsening kinetics was found in Al-Zr-Sc alloys [3,4]. However, the high cost of scandium limited its commercial use and elements with lower cost are welcomed in engineering applications.

Y locates in the same group as Sc, however, Al_3Y was used to be regarded impossible to be effective nuclei for $L1_2$-Al_3Zr of conventionally cast Al-Zr-Y alloys [9], because the $L1_2$-Al_3Y was accessible only during the decomposition of rapid solidified Al-Y alloys [10]. Few publications could be found focusing on the precipitation evolution of Al-Zr-Y alloys. Our previous research showed that, compared with binary Al-Zr alloy, incubation time for Al-Zr-Y shortened obviously, and the number density of the precipitates is about one order magnitude higher. The width of PFZ in Al-0.3Zr-0.08Y near the grain boundary narrowed for 10–20 μm to 6–12 μm and the recrystallization temperature increased from 350 °**C** to 450 °**C** [11,12]. In present work, precipitation evolution of Al-Zr-Y alloy was further investigated through atom probe tomography (APT), transmission electron microscopy (TEM) and first principles calculations.

2. Experimental and Calculation Methods

Al-Zr-Y ingots were cast from 99.99 at.% pure Al with Al-Y and Al-Zr master alloys using alumina crucibles at 750 °**C** in the open air. The melt was poured into a graphite mold after mechanical stirring. Composition of alloys was measured by inductively coupled plasma-atomic emission spectroscopy (ICP-AES). Specimen was aged at 350 °**C** for 10 min, 400 °**C** for 2 h and 200 h to investigate the evolution of the precipitates. Transmission electron microscopy (TEM) was performed on a JEM 2100F microscope operated at 200 kV. TEM specimens were prepared through mechanical grinding and twin-jet electro-polishing at 12 V with a 30% nitric acid and 70% methanol solution cooled to −30 °C. Atom probe tomography (ATP) analyses with 200 kHz pulse repetition rate, 20% pulse fraction, 20 K specimen temperature and a residual pressure of 10^{-8} Pa was used to investigate the formation and evolution of the precipitates. Specimen with tip radii less than 100 nm were prepared through electro-chemical polishing. IVASTM software were employed for data processing.

First principles calculations were performed for further investigation on the distribution of Y atoms. The calculation was conducted with

* Corresponding author at: State Key Laboratory of Metal Matrix Composites, Shanghai Jiao Tong University, Shanghai 200240, China.
E-mail addresses: gaohaiyan@sjtu.edu.cn (H. Gao), junwang@sjtu.edu.cn (J. Wang).

http://dx.doi.org/10.1016/j.matchar.2016.10.012
1044-5803/

Vienna Ab initio Simulation Package. Density functional theory (DFT) at T = 0 K calculations using the plane-wave total-energy methodology with generalized gradient approximation (GGA) for exchange–correlation is implemented in the software [13–16]. Two supercells 2 × 2 × 2 and 3 × 3 × 3 were built to simulate the decomposition process. Atomic positions as well as unit-cell volume and shape were fully relaxed with respect to the volume, cell vectors and internal atomic positions. The *k*-points were set as 12 × 12 × 12 for the 2 × 2 × 2 supercell, and 4 × 4 × 4 for the 3 × 3 × 3 supercell. Energy cutoff of 320 eV gives binding energy converged to within 0.01 eV.

3. Results and Discussions

3.1. Nucleation of Al_3Y

Fig. 1 gives APT reconstruction image of Y and Zr for Al-0.30Zr-0.08Y aged at 350 °C for 10 min and the nearest neighbor distribution of Zr. APT reconstruction revealed that Y containing precipitate had formed and the precipitate is not spherical but short-bar-shaped, which indicates that the precipitate is not of a cubic structure. Distribution of Zr atoms is almost random, indicating that most of Zr atoms are still in solid solution. Fig. 2 displays the concentration profiles across the matrix/precipitate interface with an enlarged image of the reconstructed precipitate inserted. The precipitate is about 12 nm in length and 3 nm in width and height. Both Zr and Y contents increased with the increasing distance from the interface. The inner precipitate consists of about 70 at.% Al, 23 at.% Y and 7 at.% Zr, which indicates that the precipitates should be Al_3Y in the early stage of decomposition. Metastable $L1_2$-Al_3Y was only reported during the decomposition of rapid solidified Al-Y alloy so far [10]. In our experiment, the cooling rate during solidification is measured at about 18 °C/s. Therefore, Al_3Y precipitates should be of $D0_{19}$ structure according to Al-Y phase diagram. Although segregation of Zr is not obvious on the whole, Zr concentration is much higher in the precipitate than in the matrix. Concentration evolution of Zr in the precipitate is in positive correlation to that of Y, which means that precipitation of Zr may link to or accelerated by Y.

3.2. Growth and Coarsening of $Al_3(Zr,Y)$

Fig. 3 gives the concentration profile for Al-0.25Zr-0.08Y aged at 400 °C for 2 h and Fig. 4 shows the TEM image of the precipitates. Segregation of Zr atoms is noticeable at this moment and concentration of Zr reached about 25 at.%. However, the content of Y decreased from 25 at.% to about 3 at.%. What's important, the content of Zr and Y increased with increasing distance from the interface, as illustrated in Fig. 2, which is different from other RE containing Al-Zr-RE alloy, where segregation of Zr at the matrix/precipitate interface is obvious and "Al_3RE core-Al_3Zr shell" structure formed during aging. The

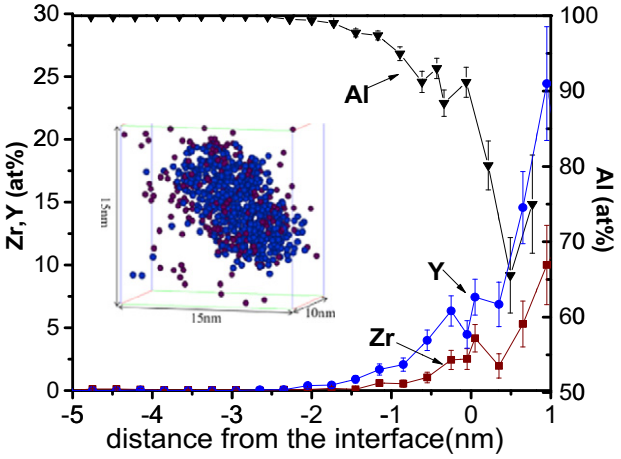

Fig. 2. Concentration profiles across the matrix/precipitate interface with a precipitate inserted in Al-0.30Zr-0.08Y aged at 350 °C for 10 min.

Ashby-Brown strain contrast in the TEM image shown in Fig. 4 indicates the precipitates are coherent with the matrix. The inserted dark field TEM image and the selected area diffraction pattern (SADP) revealed that the precipitates are spherical with $L1_2$ structure. Our previous research also found that the precipitates are composed of Al, Zr and Y atoms with EDS analysis [11].

Figs. 5 and 6 give the concentration profile and the corresponding TEM image for Al-0.25Zr-0.08Y aged at 400 °C for 200 h respectively. APT reconstruction image revealed that most of Zr and Y atoms had entered into the precipitate. However, the content of Zr and Y in the precipitates is about 23 at.% and 2 at.%, respectively, which is almost unchanged compared with that aged at 400 °C for 2 h. The results showed that Al_3(Zr,Y) should have formed after 2 h aging and a quasi-static coarsening happened as the aging treatment lasted to 200 h. It is worth noticing that after 2 h aging, morphology of the precipitate had transformed from the very beginning short bar to roundish and Al_3(Zr,Y) do not have the typical "Al_3RE core-Al_3Zr shell" structure which observed in other RE containing Al-Zr-RE alloy with a $L1_2$-Al_3RE as nucleus.

3.3. Co-Precipitation Mechanism of Zr and Y

Based on the above analyses, we can reach the conclusion that $D0_{19}$-Al_3Y precipitates were the nuclei of $L1_2$-Al_3Zr, and due to the formation of $L1_2$-Al_3Zr, morphology of the precipitate also transformed into spherical gradually. Lattice parameter of (111) in $L1_2$-Al_3Zr is 3.09, which is just half of that of (001) in $D0_{19}$-Al_3Y. That is, coherent interface

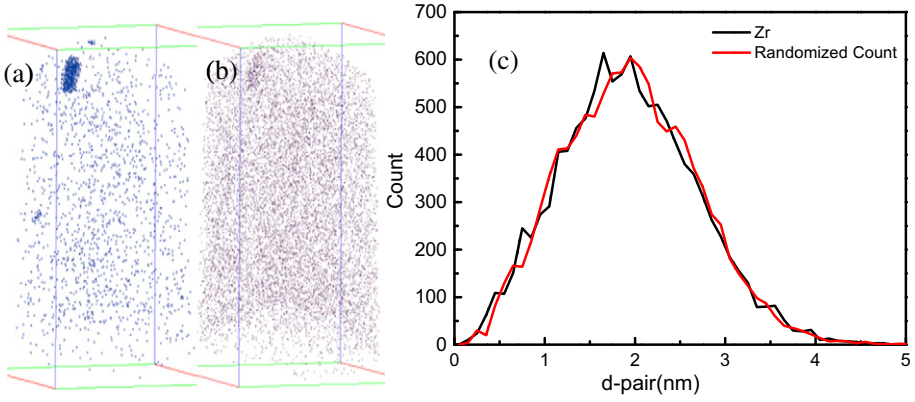

Fig. 1. APT reconstruction for Y atoms (a) and Zr atoms (b) for Al-0.30Zr-0.08Y aged at 350 °C for 10 min and the nearest neighbor distribution of Zr atoms (c). Distribution of Zr atoms is almost random while segregation of Y is obvious.